Spin assignments of angular momentum mismatched resonances in the $^{16}O+^{16}O$ system

S. P. Barrow, R. W. Zurmühle, A. H. Wuosmaa,* and S. F. Pate†
Physics Department, University of Pennsylvania, Philadelphia, Pennsylvania 19104
(Received 21 May 1992)

Detailed angular distributions for the reaction $^{16}O(^{16}O,^{16}O(0_2^+,6.05\ MeV))^{16}O(g.s.)$ were obtained for nine center of mass energies varying from 25.5 to 35.5 MeV. From these angular distributions a dominant partial wave is assigned to three of the gross resonances in this system. The spin assignments are consistent with a rotational sequence, and are in disagreement with the results of a previous study of the same reaction.

PACS number(s): 25.70.Ef

I. INTRODUCTION

Resonant structure in angular momentum mismatched reactions has generated a large amount of theoretical and experimental work. A system that is extremely well suited to study momentum mismatching is the $^{16}O(^{16}O,^{16}O(0_2^+,6.05\ MeV))^{16}O(g.s.)$ system, as the spinless excited state eliminates the complication of coupling intrinsic and orbital momenta. In addition, the use of identical particles removes odd partial waves from the cross section, which increases the energy spacing between peaks and facilitates the assignment of spins to the resonances.

Theoretical efforts to explain mismatched resonances utilize coupled channel calculations, where both strong and weak coupling schemes have been considered. Weak coupling schemes are based on the band-crossing model. Early versions of this model implemented an angular momentum matching condition in which a negative Q value was compensated for by a smaller value of the orbital angular momentum, but this picture is unable to describe the resonance behavior for transitions such as to the 0_2^+ state in ^{16}O. Langanke, Friedrich, and Koonin [1] introduced two bands: a "shape resonance" and a "molecular state" band. In this model the shape resonance in the elastic channel is matched with the molecular band in the 0_2^+ channel at resonant energies. Attempts were also made to explain the resonances by increasing the strength of the channel coupling [2].

Balamuth *et al.* [3] undertook the first exclusive study of the $^{16}O(^{16}O,^{16}O(0_2^+,6.05\ MeV))^{16}O(g.s.)$ reaction channel. They reported angular distribution measurements over an angular range between 55° and 90° at 65 beam energies. These measurements confirmed the presence of strong gross structures that were suggested by an earlier inclusive measurement [4], as well as narrower, weaker structures. The narrow structures appear as weak fluctuations on the smoothly varying gross structures in the angle integrated excitation function. The limited angular range precluded an analysis of the angular distributions in terms of fits to partial waves. Instead, the authors performed a zeros analysis, which is a study of the energy dependence of the function

$$Z_l(E)=2\pi\sum_{i=1}^{N}\int_{\theta_i-\Delta\theta/2}^{\theta_i+\Delta\theta/2}\sigma(E,\theta')\sin(\theta')d\theta' \ . \qquad (1)$$

This expression consists of a sum of integrals of the differential cross section over narrow angular regions centered at the zeros of the Legendre polynomial of degree l. If only one l value contributes to each resonance that spin value is readily identified by the absence of structure in the zeros analysis for that Legendre polynomial at the resonant energies. Spin assignments of $l=16,18,22,24$ emerged from the zeros analysis for the excitation function peaks at $E_{c.m.}=25.6$, 29.3, 33.6, and 38.2 MeV, respectively. The absence of $l=20$ is particularly disturbing since the spins are not consistent with a rotational sequence. Balamuth *et al.* [3] speculated that the $l=20$ strength might be more fragmented than the other resonances.

II. EXPERIMENT

In the present work we have reexamined this reaction to learn more about the partial waves that dominate the structures in the energy region of the unidentified $l=20$ strength. In order to supplement the existing data we decided to measure detailed angular distributions over the widest possible angular range at a few carefully chosen energies. Angular distributions for $7°\le\theta_{c.m.}\le 93°$ were measured for nine c.m. energies ranging from 25.5 to 35.5 MeV. Events were recorded by requiring a coincidence between an ^{16}O nucleus and an electron or positron from the 0_2^+ decay pair. This coincidence requirement effectively reduced background effects from the nearby 3^- state. A major concern was the rate at which gammas from the 3^- decay would produce electrons which would then be detected by the electron detector. The most likely source of these false events is instances in which the gammas interact with the 0.0254 cm thick aluminum foil

*Present address: Argonne National Laboratory, Argonne, IL 60439.
†Present address: MIT, Cambridge, MA 02139.

which covers the electron detector. (The aluminum housing is described in more detail below.) However, we calculated that only 0.2% of the gammas that pass through the aluminum foil create electrons, which is an acceptable amount for our purposes. This estimate neglects the interactions of the gammas with the walls of the scattering chamber, and therefore has to be considered a lower limit, but evidence of the success of the 3^- suppression comes from the angular distributions which have clear oscillations. The energy of the ^{16}O nucleus was used to differentiate single excitations of the 0_2^+ state from other inelastic processes such as mutual excitations and many body final states.

For $\theta_{c.m.} \geq 30°$ a gas-silicon detector telescope [5] was used to detect and identify the inelastically scattered ^{16}O nuclei. The silicon detector was divided into 50 slices with an angular acceptance of 0.7° per slice. Members of the e^+-e^- decay pairs were detected using a 450 mm^2 300 μm thick partially depleted solid-state detector enclosed in an aluminum housing 0.0254 cm thick, which shielded the detector from heavier charged particles. The electron detector was placed 1.0 cm from the target and covered about 30% of 4π. To minimize noise contributions from leakage current the detector and the telescope were operated at −20° C. Two monitor detectors positioned at 10° on either side of the beam were used to normalize the cross sections. For the measurements at angles smaller than 30° a magnetic spectrograph was used, and an anthracene crystal with a large surface area coupled to a fast photomultiplier [6] was used to detect the e^+-e^- decay pair. It proved to be very difficult to measure the angular distributions forward of 3° in the laboratory system due to the background from the scattered and energy degraded beam. An ^{16}O beam from the Tandem accelerator at the University of Pennsylvania bombarded 25 $\mu g/cm^2$ BeO foils, which corresponds to an energy loss of 100 keV in the center of mass system for these beam energies. There are several advantages in using BeO targets over the more conventionally used oxides of Al, Si, or Ta. They can withstand very high beam intensities, and, because the presence of beryllium in the target adds very little to the counting rates in the detectors, data can be acquired with these intensities. We found it difficult, however, to make these targets significantly thicker than the above value.

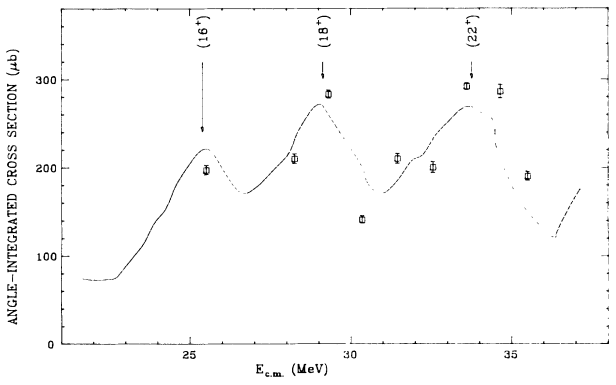

FIG. 1. The cross sections from the present work are plotted individually, while the solid line is a reproduction of the excitation function of Ref. [3]. The cross sections are integrated between 55° and 90° in the c.m. frame. The excitation function of Ref. [3] was energy averaged with a 1.5 MeV square averaging interval in order to display the gross structures more clearly. Also shown are the spin assignments of Ref. [3] for the three resonances.

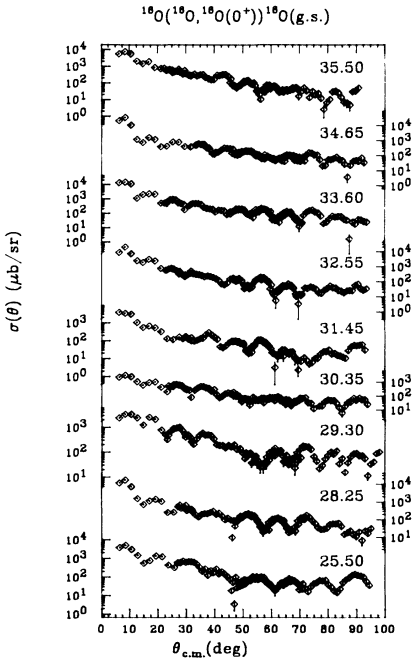

FIG. 2. Angular distributions from the present work. The center of mass energy (in MeV) is given above each distribution. The error bars are statistical.

Angle-integrated cross sections as a function of $E_{c.m.}$ for the angle range 55°–90° are shown in Fig. 1. The energy averaged, angle-integrated excitation function from Ref. [3] for the same angle range is also plotted in Fig. 1. (The excitation function of Ref. [3] without the energy averaging has appeared in the literature elsewhere [7].) The angular distributions from the present work are shown in Fig. 2. We chose to concentrate on the energy range from 28.25 to 35.5 MeV where the 29.3 and 33.6 MeV structures are located, but we also made a measurement at 25.5 MeV where the lowest lying structure peaks.

III. ANALYSIS

Our nine point excitation function contains enough data for a zeros analysis for the peaks centered at 29.3 and 33.6 MeV. The zeros analysis of Ref. [3] included an energy averaging of the angular distributions. By averaging over an energy region larger than the widths of the narrow structures yet smaller than or comparable to the widths of the gross structures, the fluctuations are averaged out and their importance to the angular distributions diminished. For the small angular range of Ref. [3]

the energy averaging is important, for as is quantified by the concept of coherence angle, the significance of the fluctuations is increased as the angular range of the data is reduced. The energy averaging of Ref. [3] was done using 1.5 MeV square averaging intervals, but due to the roughly 1 MeV spacing between adjacent energies in our excitation function we do not have a sufficiently high density of points to apply such energy averaging to our data. A thicker BeO target could eliminate the need for any energy averaging, but currently no way is known to produce targets as thick as 800 keV (the approximate half width at half maximum of the gross structures.) However, we can substantially reduce the influence of the fluctuations by summing over many zeros of the Legendre polynomial of interest. Averaging washes out any possible local l dominance from the narrow structures which might complicate the analysis for any given angle, and the present work contains data for $(L/2)-1$ zeros for each partial wave we studied, as opposed to four or five zeros for the angular range of Ref. [3]. The fluctuations should therefore have a correspondingly smaller effect on the current zeros analysis.

The results of the zeros analysis performed on the present angular distributions are shown in Fig. 3, and they indicate that the choice of angular range has a strong effect on the conclusions. The analysis shown in Figs. 3(d)–3(f) uses data in the angular range $\theta=55°-90°$, and is in reasonable agreement with the results of Ref. [3], which uses the same angular range but with energy smoothed data. From these figures, it would seem that $l=18$ is a reasonable choice for the resonance at 29.3 MeV and $l=22$ for the structure at 33.6 MeV. The zeros analysis for the entire angular range is presented in Figs. 3(a)–3(c). Here $Z_{18}(E)$ shows a pronounced structure at 29.3 MeV, which would seem to rule out an $l=18$ assignment for this structure. In contrast $Z_{20}(E)$ shows a rather smooth energy dependence, and is therefore the more likely choice for the spin of this resonance. The absence of structure in the zeros functions at resonant energies is not nearly as complete as one would like it to be. This effect was also observed and commented on in Ref. [3].

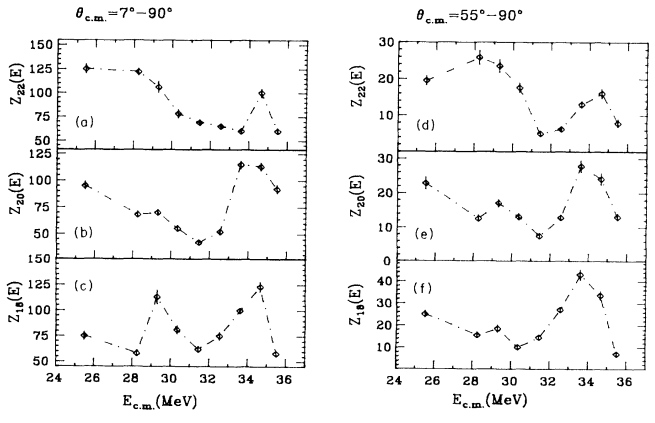

FIG. 3. Zeros analysis for two different angle ranges. (a)–(c) include data from our entire angle range. (d)–(f) include data from the same angle range, 55°–90°, used in Ref. [3]. The lines joining adjacent points are provided to guide the eye.

It is clear from the above discussion that the zeros analysis is sensitive to the choice of angular range. Such sensitivity makes it difficult to draw any strong conclusions from the zeros analysis results. We therefore decided to try two other approaches: linear expansions of the angular distributions and fits to a coherent sum of several surface partial waves. With the large angular range of the current work, such procedure are more feasible than for the smaller angular range of Ref. [3].

We first tried fitting the angular distributions by a linear Legendre expansion [8] to extract the resonating partial wave for each resonance. Due to the fact that we had no data from 0° to 7°, and that points in the angular distributions were not evenly spaced, this method did not work well. The expansions frequently gave meaningless results, such as a negative cross section at small angles or a negative coefficient for the largest partial wave. Given the difficulties inherent in acquiring additional data at smaller angles we abandoned this approach.

We then tried fitting the angular distributions by a sum of surface partial waves. The angular distributions were fitted by the usual expression for scattering of spinless particles:

$$\sigma(\theta,E)=\left|\sum_l A(l,E)e^{iB(l,E)}P_l(\cos\theta)\right|^2 , \tag{2}$$

where for identical particles the sum is only over even l values. Although such fits are not unique, they serve to illustrate the l dependence of the cross sections. As the models predict one partial wave accounting for each resonance, and, as the peak-to-background ratio for each resonance is roughly two-to-one, we decided to only accept fits in which a dominant partial wave accounts for at least 40% of the cross section. The narrow structures are too weak to influence the coefficients significantly, they could only manifest themselves as small fluctuations in the amplitudes and phases of the fits and have no bearing on the discussion which follows.

Fits were obtained using the fitting routine MINUIT [9]. The coefficients from the fits were expressed in the form used in Eq. (2):

$$A(l,E)e^{iB(l,E)} . \tag{3}$$

In each fit, the phase of one coefficient is set to zero, and all other phases are defined relative to the first. The software allowed the initial values of the coefficients to be varied, as well as the step size and the number of iterations of the search, and all these parameters were varied to try to find the best fits. A typical fit utilized a dozen or so parameters. One method was to arrange the initial conditions such that one Legendre polynomial had a large coefficient. This was then repeated for many l values. In so doing, each l value was given a change to dominate a fit, which was a good way to determine which l values are preferred by the data. Another approach was to input initial conditions which were assumed to be near the actual values, to see if MINUIT would find better fits than it did with the first method. For the most part, these two approaches produced the same fits. Many

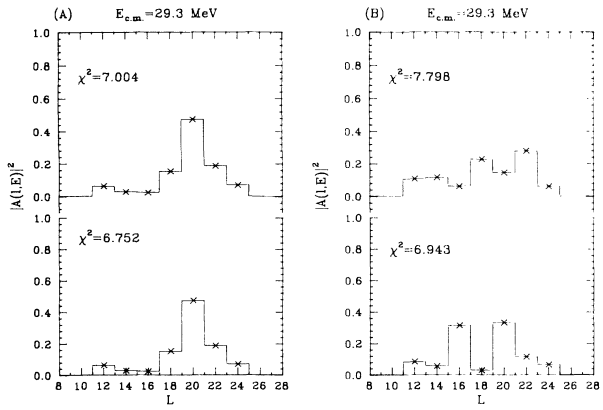

FIG. 4. The squares of the magnitudes of the MINUIT generated coefficients are plotted. The sum of the squares is normalized to 1.0. (a) contains plots which are consistent with a single resonating partial wave accounting for the resonance, (b) shows fits in which the cross section is fragmented over several partial waves, which is not consistent with the picture of a single partial wave dominating the peak. These fits are therefore rejected. The error bars for the coefficients are too small to be visible.

different sets of l values were tried. Sets ranging in size from three consecutive to seven consecutive even Legendre polynomials were tried. Usually these sets were centered around $l=18$ or 20, but fits were also tried with $l=18$ or 20 comprising either the high l or low l portion. Several dozen variations were tried for the energies 25.5, 29.3, 33.6, and 34.65 MeV, and all energies were subjected to standardized fits. Examples of both rejected and accepted fits are shown in Fig. 4. The quality of the fits is independent of this condition as the χ^2 of the fits in Fig. 4 demonstrates.

IV. RESULTS

A. $E_{c.m.}=33.6$ MeV

We performed our fits on the angular distribution data for 33.6 MeV, and seven of the fits met the criterion. Of these seven, five had $l=22$ as the dominant partial wave, while the other two had $l=26$. Figure 5(a) shows a fit for which $l=22$ is the dominant partial wave. It is apparent that the three forward points are not well fitted, but that they could be reproduced much better with a fit containing higher partial waves. Repeating the fitting procedure without the three forward angles drastically reduces χ^2 and eliminates the need for an $l=26$ partial wave. Such strong dependence on three forward angles may indicate that our description of the nonresonant background is flawed, and that $l=26$ is not the resonating partial wave, but this is not a strong enough reason to reject the $l=26$ fits.

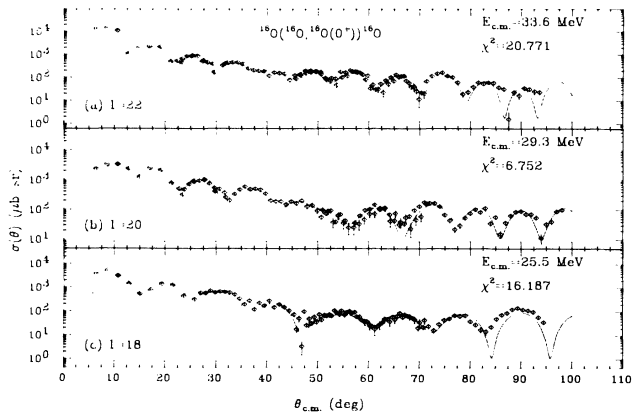

FIG. 5. Fits to the angular distributions of the three resonant energies. Each fit shown has a dominant partial wave with at least 40% of the total cross section. The dominant partial waves are $l=18$, 20, and 22 for $E_{c.m.}=25.6$, 29.3, and 33.6 MeV, respectively.

B. $E_{c.m.}=29.3$ MeV

For 29.3 MeV, once again two l values meet the criterion: $l=20$ and $l=22$. Five different fits were generated, four with $l=20$, one with $l=22$. For this energy, as was the case for 33.6 MeV, it is not possible to eliminate one partial wave. However, as is readily seen in Fig. 4(a), the coefficient of $l=18$ is consistently well below the strength required for the resonating partial wave, which is strong evidence for ruling out $l=18$. Once $l=18$ is eliminated, the zeros analysis of Fig. 3(b) suggests $l=20$ as the most suitable, but both $l=20$ and $l=22$ must remain candidates. A fit with $l=20$ as the dominant partial wave is shown in Fig. 5(b).

C. $E_{c.m.}=25.5$ MeV

The analysis for 25.5 MeV is the most direct of the three. Every fit, such as the one shown in Fig. 5(c), with a single dominant partial wave had $l=18$ as the dominant wave, and therefore this resonance is assigned a spin of $l=18$.

V. SUMMARY AND CONCLUSION

The analysis based on an expansion of the angular distributions into coherent sums of surface partial waves reduces the choice of acceptable spin values for the three structures at 25.5, 29.3, and 33.6 MeV to $l=18$, {20 or 22}, and {22 or 26}, respectively. The assumption of a single dominant partial wave that was made at the outset is crucial to this conclusion because good fits with small contributions from several partial waves have also been obtained.

Our results are in disagreement with the results of Ref. [3] for the resonances at 25.5 and 29.3 MeV, but they are consistent with their assignment of $l=22$ for $E_{c.m.}=33.6$. The discrepancies can be attributed to limitations of the zeros analysis when only a small portion of the angular distribution is studied. This effect was clearly manifest in our zeros analysis, which produced contradicting results for different angular regions of the same resonance. It is encouraging that the spin assignments of the present work are consistent with a rotational sequence, and that the missing $l=20$ resonance has been found.

Out of the current spin assignments, only one set of spins consistent with a rotational sequence can be

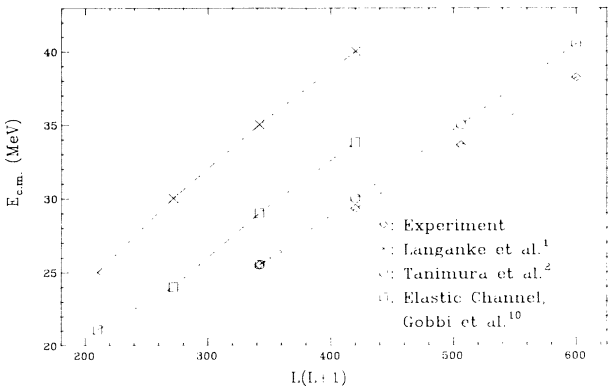

FIG. 6. The spin assignments of the present work yield only one set which is consistent with a rotational sequence. This set is $4\hbar$ larger than the predictions of Ref. [1] and $2\hbar$ larger than the elastic scattering calculations of Ref. [8]. The spins are in qualitative agreement with Ref. [2]. The spin assignment of $l=24$ for $E_{c.m.}=38.2$ MeV from Ref. [3] has been included.

formed, and this new spin sequence is $4\hbar$ higher than the spins predicted by the weak coupling model of Ref. [1]. The new spins are in qualitative agreement with the strong coupling calculations of Ref. [2], and, as is seen in Fig. 6, the spins are higher than the spins from an optical model calculation [10] for the $^{16}O+^{16}O$ elastic channel. This is an intriguing result, given that other systems in this mass region have resonances with spins larger than the grazing angular momentum [11], and it suggests that these resonances may correspond to the formation of nuclear molecules consisting of one ^{16}O nucleus in the strongly deformed (0_2^+, 6.05 MeV) state. Additional experiments such as an exclusive study of mutual excitation to the 0_2^+ state would be a fruitful way to study this phenomena further, and we are planning to do such an experiment in the near future.

ACKNOWLEDGMENTS

We would like to acknowledge the assistance of D. A. Smith, C. M. Laymon, G. B. M. Vaughan, and J. C. Satterthwaite in the analysis of the data. We would like to thank D. P. Balamuth for providing data to us. We would like to thank D. P. Balamuth, H. T. Fortune, J. T. Murgatroyd, and N. G. Wimer for helpful discussions. This work was supported by the National Science Foundation.

[1] K. Langanke, H. Friedrich, and S. E. Koonin, Phys. Rev. Lett. **51**, 1231 (1983).
[2] O. Tanimura and U. Mosel, Phys. Rev. C **24**, 321 (1981).
[3] D. P. Balamuth, T. Chapuran, C. M. Laymon, W. K. Wells, and D. P. Bybell, Phys. Rev. Lett. **55**, 2842 (1985).
[4] W. S. Freeman, H. W. Wilschut, T. Chapuran, W. F. Piel, Jr., and P. Paul, Phys. Rev. Lett. **45**, 1479 (1980).
[5] R. Zurmühle and L. Csihas, Nucl. Instrum. Methods **203**, 261 (1982).
[6] W. Wells, D. Cebra, and D. Balamuth, Nucl. Instrum. Methods **223**, 103 (1984).
[7] S. F. Pate, R. W. Zurmühle, A. H. Wuosmaa, P. H. Kutt, M. L. Halbert, D. C. Hensley, and S. Saini, Phys. Rev. C **41**, R1344 (1990).
[8] J. R. Hurd, N. R. Fletcher, A. D. Frawley, and J. F. Mateja, Phys. Rev. C **22**, 528 (1980).
[9] F. James and M. Roos, Comput. Phys. Commun. **10**, 343 (1975).
[10] A. Gobbi, R. Wieland, L. Chua, D. Shapira, and D. A. Bromley, Phys. Rev. C **7**, 30 (1973).
[11] A. H. Wuosmaa, R. W. Zurmühle, P. H. Kutt, S. F. Pate, S. Saini, M. L. Halbert, and D. C. Hensley, Phys. Rev. C **41**, 2666 (1990).